View metadata, citation and similar papers at core.ac.uk

brought to you by CORE

provided by Elsevier - Publisher Connector

Translational Oncology
www.transonc.com

Volume 9 Number 5 October 2016 pp. 403–410 403

# Diffusion-Weighted Imaging Using a Readout-Segmented, Multishot EPI Sequence at 3 T Distinguishes between Morphologically Differentiated and Undifferentiated Subtypes of Thyroid Carcinoma—A Preliminary Study

**Stefan Schob[*], Peter Voigt[‡], Lionel Bure[¶], Hans-Jonas Meyer[§], Claudia Wickenhauser[†], Curd Behrmann[§], Annekathrin Höhn[**], Paul Kachel[#], Henning Dralle[#], Karl-Titus Hoffmann[*] and Alexey Surov[‡]**

*Department of Neuroradiology, University Leipzig, Leipzig, Germany; [†]Department of Pathology, Martin Luther University Halle-Wittenberg, Leipzig, Germany; [‡]Department of Diagnostic and Interventional Radiology, University Leipzig, Leipzig, Germany; [§]Department of Diagnostic Radiology, Martin Luther University Halle-Wittenberg, Leipzig, Germany; [¶]Department of Radiology, McGill University Health Center, Montreal General Hospital, Quebec, Canada; [#]Department of General, Visceral and Vascular Surgery, Martin Luther University Halle-Wittenberg, Leipzig, Germany; **Department of Pathology, University Leipzig, Leipzig, Germany

## Abstract

*BACKGROUND:* Thyroid carcinomas represent the most frequent endocrine malignancies. Recent studies were able to distinguish malignant from benign nodules of the thyroid gland with diffusion-weighted imaging (DWI). Although this differentiation is undoubtedly helpful, presurgical discrimination between well-differentiated and undifferentiated carcinomas would be crucial to define the optimal treatment algorithm. Therefore, the aim of this study was to investigate if readout-segmented multishot echo planar DWI is able to differentiate between differentiated and undifferentiated subtypes of thyroid carcinomas. *PATIENTS AND METHODS:* Fourteen patients with different types of thyroid carcinomas who received preoperative DWI were included in our study. In all lesions, apparent diffusion coefficient (ADC)min, ADCmean, ADCmax, and *D* were estimated on the basis of region of interest measurements after coregistration with T1-weighted, postcontrast images. All tumors were resected and analyzed histopathologically. Ki-67 index, p53 synthesis, cellularity, and total and average nucleic areas were estimated using ImageJ version 1.48. *RESULTS:* Analysis of variance revealed a statistically significant difference in ADCmean values between differentiated and undifferentiated thyroid carcinomas ($P = .022$). Spearman Rho calculation identified significant correlations between ADCmax and cell count ($r = 0.541$, $P = .046$) as well as between ADCmax and total nuclei area ($r = 0.605$, $P = .022$). *CONCLUSION:* DWI can distinguish between differentiated and undifferentiated thyroid carcinomas.

*Translational Oncology (2016) 9, 403–410*

## Introduction

Carcinomas of the thyroid gland represent the most frequent malignancies of the endocrine system. The incidence rate of thyroid cancer is increasing worldwide, and the disease mainly affects young to middle-aged adults [1]. Most thyroid neoplasms are differentiated thyroid carcinomas (DTCs) derived from follicular epithelial cells, and among these, papillary thyroid carcinomas (PTCs) account for

Address all correspondence to S. Schob, Department of Neuroradiology, University Leipzig, Leipzig, Germany.
E-mail: stefan.Schob@medizin.uni-leipzig.de
Received 17 August 2016; Revised 29 August 2016; Accepted 1 September 2016

© 2016 The Authors. Published by Elsevier Inc. on behalf of Neoplasia Press, Inc. This is an open access article under the CC BY-NC-ND license (http://creativecommons.org/licenses/by-nc-nd/4.0/).
1936-5233/16
http://dx.doi.org/10.1016/j.tranon.2016.09.001

90% of all thyroid carcinomas, whereas follicular thyroid carcinomas (FTCs) represent 5% to 15% of all thyroid carcinomas. Medullary thyroid carcinomas (MTCs, arising from the parafollicular C-cells) and undifferentiated thyroid carcinomas (UTCs) account for 5% and 2% of all thyroid carcinomas, respectively. Patients with DTCs have excellent survival rates, usually longer than 20 years after the initial diagnosis, whereas MTCs and UTCs are associated with a far worse prognosis [1,2]. Thus, therapeutic strategies for DTCs differ significantly from poorly differentiated carcinomas like UTCs and MTCs [3].

The classical subdivision of thyroid malignancies, namely, papillary, follicular, medullary, and undifferentiated carcinomas, is strongly supported by molecular studies revealing the participation of specific genes with little overlap [4–7]. Although the majority of thyroid carcinomas can be classified using the four aforementioned morphology-based categories, there are few carcinomas which have features of more than one classic histopathological subtype. These tumors reveal a distinct tumor biology and therefore a variable outcome [1].

For example, the follicular and tall cell variants of PTCs present with a diverse outcome, yet they are both categorized as PTCs [1]. Hürthle cell carcinoma is another example of that discrepancy, as it represents the oxyphilic subtype of FTCs, which is also associated with a worse prognosis than standard FTCs [1].

Considering the relevance of the histopathological tumor subtypes for optimal treatment planning, supplementary diagnostic approaches with the ability to separate more indolent lesions which would necessitate less radical therapies from more aggressive tumors requiring extensive resection and adjuvant therapies are necessary.

Magnetic resonance imaging (MRI), especially diffusion-weighted imaging (DWI), has been used as a surrogate marker of increased mitotic activity to identify aggressive features in several tumors [8]. In particular, different components of the apparent diffusion coefficient (ADC) have been shown to predict increased proliferation rates and areas of high cellularity in benign and malignant masses [9,10].

Based on the principle that DWI is able to distinguish tumors with different cellular architecture, recent studies showed that DWI has the potential to separate malignant and benign thyroid nodules [11–13]. The commonly used single-shot EPI sequences are prone to susceptibility and blurring artifacts especially at 3 T and provide a comparatively low resolution [14]. The main goal of our study is to investigate if DWI using a readout-segmented, multishot EPI (RESOLVE) sequence—which suffers less from the abovementioned limitations—is able to differentiate between well-differentiated and undifferentiated subgroups of thyroid carcinomas. Secondary goals were to identify possible correlations of DWI biomarkers and histopathologic data like cellularity, average and total nuclei areas, as well as Ki-67 index and p53 expression.

## Material and Methods

This study was approved by the institutional review board (Martin Luther University ethic committee).

### *Patients*

Overall, 20 patients with different thyroid carcinomas were identified in our radiological database. As only 14 patients received preoperative MRI scans including DWI, these 14 patients were included into the retrospective analysis. Our group's demographics consisted of 1 woman and 13 men with a mean age of 66 years ranging from 41 to 91 years. Four patients (28.5%) suffered from FTCs, 4 patients (28.5%) from PTCs, and 6 patients (43%) from UTCs.

### *MRI*

For all patients, cervical MRI was performed using a 3.0-T device (Magnetom Skyra; Siemens, Erlangen, Germany). The imaging protocol included the following sequences:

1. Axial T2-weighted (T2w) turbo spin echo sequence [repetition time (TR)/echo time (TE): 4000/69, flip angle: 150°, slice thickness: 4 mm, acquisition matrix: 200 × 222, field of view: 100 mm]
2. Axial T1-weighted (T1w) turbo spin echo sequences (TR/TE: 765/9.5, flip angle: 150°, slice thickness: 5 mm, acquisition matrix: 200 × 222, field of view: 100 mm) before and after intravenous application of contrast medium (gadopentate dimeglumine, Magnevist; Bayer Schering Pharma, Leverkusen, Germany)
3. Axial DWI (RESOLVE sequence; TR/TE: 5400/69, flip angle 180°, slice thickness: 4 mm, acquisition matrix: 200 × 222, field of view: 100 mm) with *b* values of 0, 400, and 800 s/mm$^2$. ADC maps were generated automatically by the implemented software package. $D_{b800\_b400}$ was calculated as described previously [15].

All images were available in digital form and were analyzed by an experienced radiologist without knowledge of the histopathological diagnosis on a PACS workstation (Centricity PACS; GE Medical Systems, Milwaukee, WI). Figure 1 shows conventional MRI images (a, axial T1 without gadolinium; b, axial T1 with gadolinium; and c, axial T2) and DWI images (d, axial b0; e, axial b400; f, axial b800; and g, axial ADC).

The slices with the largest diameter of each tumor were selected for DWI measurements and subsequent ADC calculation. In every case, a polygonal region of interest as large as possible was manually drawn on postcontrast T1w images. Every region of interest was automatically coregistered on all other images (T2w and precontrast T1w, b0, b400, and b800). Cystic, calcified, and necrotic areas as well as large vessels of the lesion were avoided. In all tumors, minimal ADC value (ADCmin), mean ADC value (ADCmean), and maximum ADC value (ADCmax) were measured. Additionally, *D* values were calculated for every tumor as described previously [15].

### *Histopathology and Immunohistochemistry*

All thyroid carcinomas were surgically resected and histopathologically analyzed.

In every case, the proliferation index was estimated on Ki-67 antigen–stained specimens using MIB-1 monoclonal antibody (DakoCytomation, Denmark) as reported previously [15]. Furthermore, p53 index was estimated using monoclonal antibody p57, clone DO-7 (DakoCytomation, Denmark). Two high-power fields (0.16 mm$^2$ per field, ×400) were analyzed. The area with the highest number of positive nuclei was selected. Additionally, cell density was calculated for each tumor as average cell count per five high-power fields (×400). Furthermore, average nucleic size and total nucleic area were estimated using ImageJ package 1.48v (National Institute of Health) as described previously [15].

All histopathological sections were analyzed using a research microscope, Jenalumar, equipped with a diagnostic instruments camera (model 4.2; Zeiss, Jena, Germany). Figure 2, *a* and *b*, shows representative high-power fields of Ki-67– and p53-stained sections.

### *Statistical Analysis*

Statistical analysis was performed using SPSS Version 20. Differences between groups in DWI parameters were assessed using one-way analysis of variance (ANOVA). *Post hoc* analysis was performed using Tukey's test. Correlations between parameters of

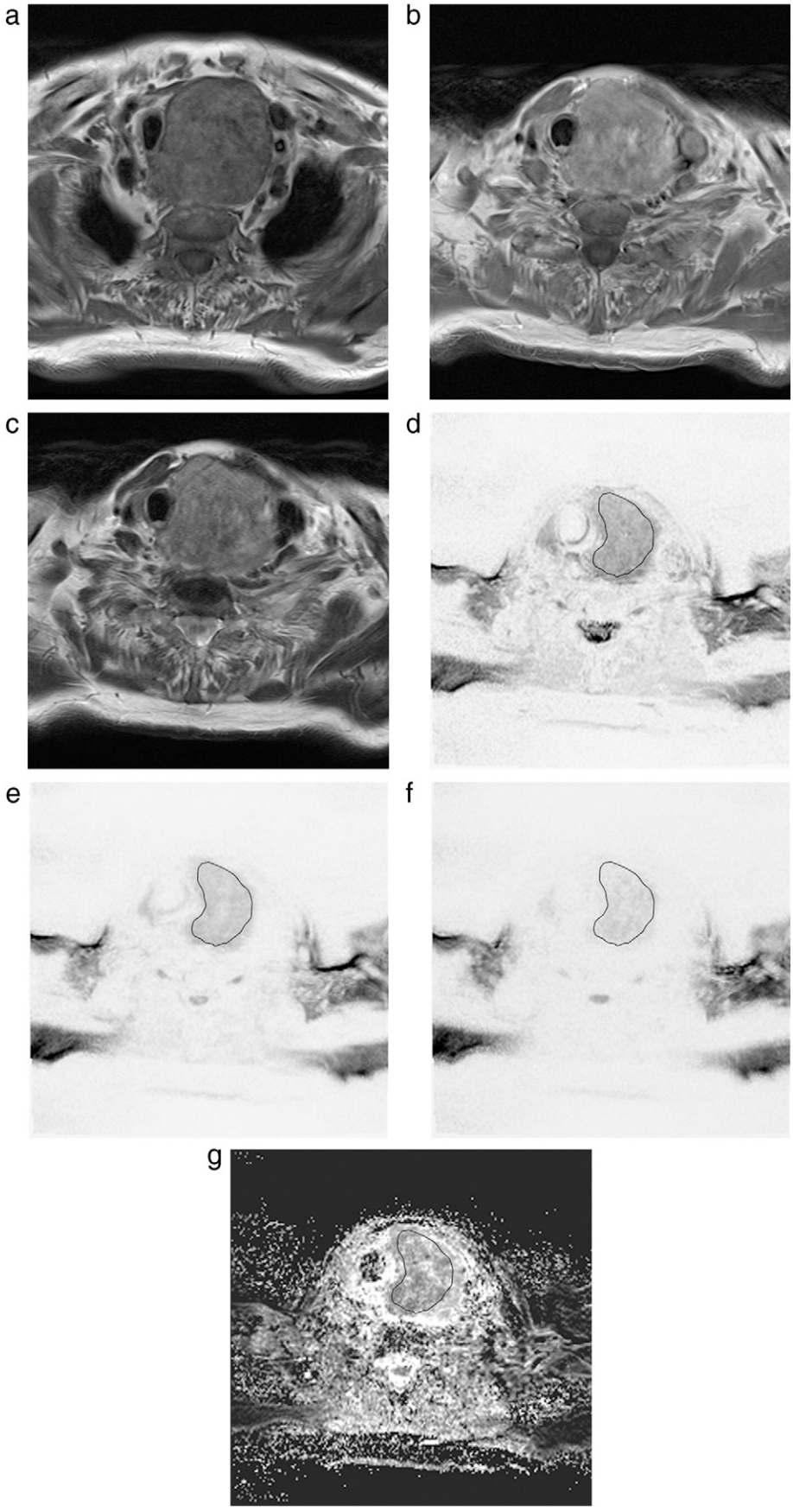


**Figure 1.** Imaging and histopathological findings in a patient with undifferentiated thyroid cancer. Magnetic resonance imaging [(a) T1w axial scan; (b) T1w axial postcontrast scan, (c) T2w axial scan] documenting a massive inhomogenous enlargement of the left thyroid lobe with infiltration of the trachea and adjacent soft tissue. On DWI, the lesion shows diffusion restriction [(d) $b = 0$; (e) $b = 400$; (f) $b = 800$; (g) ADC]. The calculated ADC values ($\times 10^{-3}$ mm$^2$ s$^{-1}$) are as follows: $ADC_{min} = 0.38$; $ADC_{mean} = 1.11$; $ADC_{max} = 1.95$. $D$ is $1.44 \times 10^{-3}$ mm$^2$ s$^{-1}$.

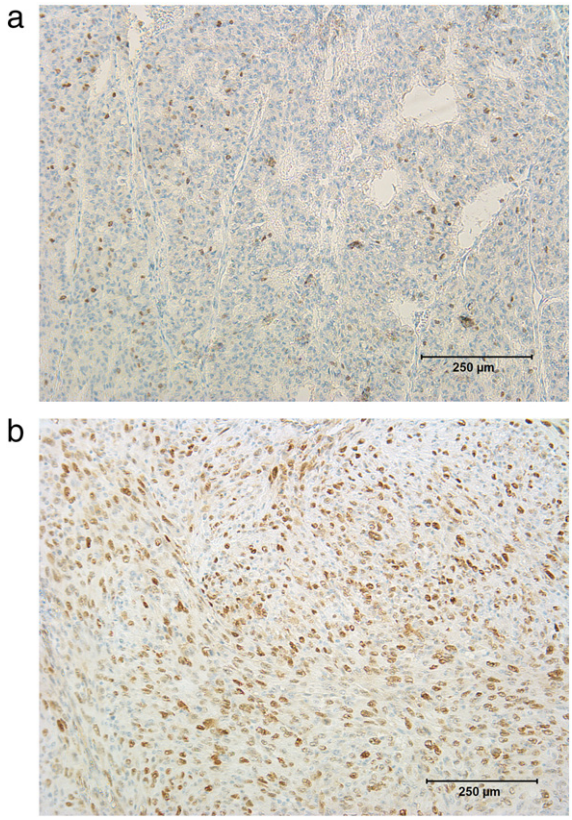


**Figure 2.** Histopathological findings [(a) Ki-67; (b) p53]. Ki-67 index = 32%, p53 = 66%.

DWI (ADCmin, ADCmean, ADCmax, $D_{b800\_b400}$) and (immuno)-histopathology (cell count, average nucleic area, total nucleic area, Ki-67 index, p53 synthesis) were calculated using a Spearman Rho correlation. Significance level was set to .05.

## Results

Estimated values of DWI of thyroid carcinomas (ADCmin, ADCmean, ADCmax, and $D_{b800\_b400}$) are shown in Table 1.

Histopathological parameters of thyroid carcinomas are summarized in Table 2.

A synopsis of the results of one-way ANOVA is given in Table 3.

Identified correlations between histopathological parameters and DWI are displayed in Table 4.

ANOVA revealed a difference between the investigated subgroups of thyroid carcinoma in ADCmean values which achieved statistical significance ($P$ = .021). A complementary box plot is shown in Figure 3*a*. Tukey's test indicated that ADCmean values are different between follicular carcinomas and undifferentiated carcinomas ($P$ = .057) as well as between papillary carcinomas and undifferentiated carcinomas ($P$ = .031). A trend of variance between subgroups was also delineable for $D_{b800\_b400}$, but ANOVA did not reach statistical significance ($P$ = .072).

Spearman Rho calculation identified statistically significant correlations between ADCmax and cell count ($r$ = 0.541, $P$ = .046) as well as between ADCmax and total nuclei area ($r$ = 0.605, $P$ = .022). Trends of correlation (without achieving statistical significance) were identified for the following pairs of parameters: ADCmean and Ki-67 index($r$ = −0.508, $P$ = .063), ADCmean and p53 synthesis ($r$ = 0.511, $P$ = .062), and ADCmin and average nuclei area ($r$ = −0.481, $P$ = .081).

## Discussion

Our aim was to study the potential role of DWI as a biomarker using a RESOLVE sequence at 3 T to distinguish well-differentiated thyroid carcinoma from UTC. Further goals were to find correlations of ADC fractions with prognostically important immunohistological parameters like proliferation rate (Ki-67 index) and p53 synthesis as well as cellularity and total and average nuclei area.

In the clinical (presurgical) setting, different modalities are approached to estimate if a thyroid lesion is of rather benign or malignant nature. Among laboratory biomarkers, exemplarily Galectin-3 (Gal-3), several imaging modalities other than MRI, like ultrasound and positron emission tomography–computed tomography (PET-CT), can be used to further strengthen the suspected diagnosis and distinguish between benign or malignant space-occupying lesions.

Gal-3 has been investigated intensively regarding its diagnostic importance in thyroid malignancies, as it is highly expressed in thyroid cancer but not normal thyroid tissue and infrequently in benign thyroid lesions [16]. Immunocytochemical studies evaluating Gal-3 expression in needle aspiration specimens revealed that Gal-3 expression levels are significantly higher in FTC compared with follicular adenoma [16]. Therefore, Gal-3 is a promising parameter for presurgical evaluation of thyroid lesions with unclear dignity. However, needle aspiration biopsy is needed to acquire tissue specimen and therefore requires a—although minimally invasive—surgical procedure with all its inherent risk factors.

Ultrasound (US) evaluation of the thyroid is well established in the standard diagnostic workup and can help to indicate probable malignancy in thyroid lesions, for example, by identification of

**Table 1.** Synopsis of DWI Parameters of Thyroid Carcinoma

| DWI Parameters | Mean ± Standard Deviation | Range |
|---|---|---|
| ADCmin, $\times 10^{-3}$ mm$^2$ s$^{-1}$ | 0.64 ± 0.3 | 0.33-1.33 |
| ADCmean, $\times 10^{-3}$ mm$^2$ s$^{-1}$ | 1.18 ± 0.36 | 0.83-1.97 |
| ADCmax, $\times 10^{-3}$ mm$^2$ s$^{-1}$ | 1.91 ± 0.50 | 1.28-2.54 |
| $D_{b800\_b400}$, $\times 10^{-3}$ mm$^2$ s$^{-1}$ | 1.18 ± 0.61 | 0.36-2.22 |

**Table 2.** Synopsis of Histopathological Parameters of Thyroid Carcinoma

| Histopathological Parameters | Mean ± Standard Deviation | Range |
|---|---|---|
| Cell count | 1268.57 ± 633.97 | 439.00-2247.00 |
| Total nuclei area, µm$^2$ | 77,309.71 ± 47,117.75 | 14,649.99-163,269.00 |
| Average nuclei area, µm$^2$ | 59.14 ± 17.24 | 33.00-94.00 |
| Ki-67 index, % | 43.21 ± 33.11 | 9.00-99.00 |
| p53 index, % | 23.94 ± 31.05 | 0.00-94.00 |

**Table 3.** Results of ANOVA Calculation of DWI Parameters from Different Histopathological Subgroups

| DWI Parameters | ANOVA $P$ value |
|---|---|
| ADCmin, $\times 10^{-3}$ mm$^2$ s$^{-1}$ | .185 |
| ADCmean, $\times 10^{-3}$ mm$^2$ s$^{-1}$ | **.021** |
| ADCmax, $\times 10^{-3}$ mm$^2$ s$^{-1}$ | .261 |
| $D_{b800\_b400}$, $\times 10^{-3}$ mm$^2$ s$^{-1}$ | *.072* |

Differences between groups achieving statistical significance are displayed in bold. Delineable trends without achieving statistical significance are displayed in italics.

**Table 4.** Synopsis of Correlations between DWI and Histopathology

| | $D_{b800\_b400}$ | ADCmin | ADCmean | ADCmax |
|---|---|---|---|---|
| Cell count | $r = -0.013$ | $r = -0.204$ | $r = 0.330$ | ***r* = 0.541** |
| | P = .964 | $P = .483$ | $P = .249$ | ***P* = .046** |
| Total nuclei area | $r = -0.013$ | $r = -0.288$ | $r = 0.290$ | ***r* = 0.605** |
| | $P = .964$ | $P = .318$ | $P = .314$ | ***P* = .022** |
| Average nuclei area | $r = -0.029$ | *r = −0.481* | $r = -0.326$ | $r = 0.185$ |
| | $P = .923$ | *P = .081* | $P = .256$ | $P = .527$ |
| Ki-67 index | $r = -0.189$ | $r = -0.160$ | *r = −0.508* | $r = -0.185$ |
| | $P = .517$ | $P = .584$ | *P = .063* | $P = .527$ |
| p53 index | $r = 0.187$ | $r = 0.059$ | *r = 0.511* | $r = 0.403$ |
| | $P = .522$ | $P = .840$ | *P = .062* | $P = .153$ |

Correlations achieving statistical significance are displayed in bold. Trends of correlations are displayed in italics.

microcalcifications, which yields specificity rates from 85% to 95% [17] US, being widely available, simple to perform, comparatively cheap, and easily combinable with fine-needle aspiration biopsy, does not involve ionizing radiation and is frequently the first choice for evaluating thyroid nodules [18,19]. However, significant limitations of thyroid US are high interrater variability, limited detection of cervical metastases, and restricted evaluation of the retrosternal space and the posterior mediastinum [20]. Despite its usefulness in the distinction of malignant versus benign thyroid lesions [17], differentiablility of DTC versus UTC has not been demonstrated and may well exceed the capabilities of the method.

Hybrid imaging techniques like PET-CT combine anatomic and metabolic imaging and have proven useful for the evaluation of thyroid lesions [21]. Most well-differentiated thyroid carcinomas are relatively slow growing and can be FDG negative [22]. Also, only 4% to 7% of DTC patients present initially with distant metastases. Therefore, the role of PET-CT in the management of patients with DTC is primarily limited to postoperative follow-up and is not indicated for initial staging purposes [23]. On the contrary, UTC lesions, weather primary or metastatic, consistently show high FDG uptake [24]. Furthermore, PET-CT is beneficial for initial staging and early evaluation of treatment response and follow-up of UTC patients [21]. However, hybrid imaging techniques come with few disadvantages. Firstly, they are accompanied by a significant radiation exposure of the patient, which cannot be justified if the lesion finally proves not to be malignant. Secondly, they are still not available regionwide, and thirdly, they are rather expensive diagnostic procedures. Considering the aforementioned, hybrid imaging in the presurgical setting is not the first choice to distinguish between malignant and benign thyroid lesions, nor is it the best option to differentiate between DTC and UTC.

MRI is mostly available regionwide, offers an excellent soft tissue contrast, is less prone to interinvestigator variability than US, and is not accompanied by radiation exposure to the patient being examined. However, the role of MRI, especially DWI, in thyroid cancer workup is controversial. Few studies were able to show that DWI provides important additional information [11,25,26], whereas other works did not find additional value in DWI [27] in the context of thyroid cancer. However, all previous reports were based on standard EPI sequences for DWI, whereas our study performed DWI by means of RESOLVE DWI.

RESOLVE DWI is less liable to susceptibility artifacts, T2* blurring, and motion-induced phase artifacts and provides higher resolution compared with standard single-shot EPI sequences [14]. Considering the small size of the thyroid (compared with other parenchymal organs) and its close proximity to the tissue air interface of the trachea, these properties are very important for exact imaging of thyroid masses and certainly enhance the quality of quantitative DWI.

In our study, ADCmean values were significantly lower in undifferentiated carcinomas compared with follicular and papillary carcinomas. To the best of our knowledge, this is the first study showing the discriminability of DTC from UTC by RESOLVE DWI. Recent studies showed the importance of DWI (using standard EPI sequences), in particular of ADC fractions, to differentiate between benign and malign thyroid nodules [11–13,26]. Another recent work from Lu and colleagues showed that PTCs with extraglandular disease manifestation had significantly lower ADC values compared with papillary carcinomas strictly confined to the thyroid gland and therefore concluded that DWI has a high potential to distinguish between PTC subtypes with different tendencies of aggressiveness [28].

Treatment of thyroid cancer is predominantly surgical [29]. Because overall mortality in thyroid cancer patients is minimal, aggressive treatments such as total thyroidectomy or lymph node dissection should be limited to very advanced disease stages because of the common surgical complications like recurrent laryngeal nerve injury or permanent hypocalcemia following removal of the parathyroid glands [3]. Surgical options range from pure observation (a corresponding scenario would be a young patient suffering from microcarcinoma who is occupationally dependent on voice use, for example, a professional vocalist), lobectomy (patient suffering from uninodular disease limited to the thyroid), and extracapsular thyroidectomy with preservation of the recurrent laryngeal nerve and parathyroid glands with additional lymph node surgery (advanced disease stage with lymph node metastases) [3,30].

Although many treatment recommendations are currently available, definitive prospective evidence to guide the thyroid surgeon is lacking in most cases. For this reason, the optimal surgical treatments to this increasingly common disease remain controversial [3].

Considering our results in the context of the aforementioned works, we were able to show not only that DWI is a useful tool to separate malign and benign thyroidal masses but that, using a RESOLVE sequence at 3 T, it can be helpful to further distinguish between morphologically well-differentiated carcinoma with less aggressive tumor biology and undifferentiated carcinoma behaving much more aggressively. This additional information about thyroid carcinoma in the preoperative setting might aid the thyroid surgeon in proper risk stratification and finding the best surgical treatment algorithm for the individual patient.

Besides differences of ADCmean values of DTC and UTC, our study revealed a trend of inverse correlation between ADCmean and Ki-67 expression, although it did not reach statistical significance. Ki-67 is a nuclear protein strictly associated with cell proliferation and widely used in immunohistopathology [31]. As demonstrated previously, increased Ki-67 expression and high cellularity in tumors are associated with decreased ADCmean values, probably based on decreased water diffusibility of the reduced extracellular space due to increased proliferation of cells [10,15,32]. In addition to that, Ki-67 has been found to be a useful indicator for poor outcome in MTC [33]. Furthermore, Ki-67 aids the discrimination of follicular adenoma and follicular carcinoma [34]. These findings corroborate the significance of ADCmean as an imaging biomarker for the

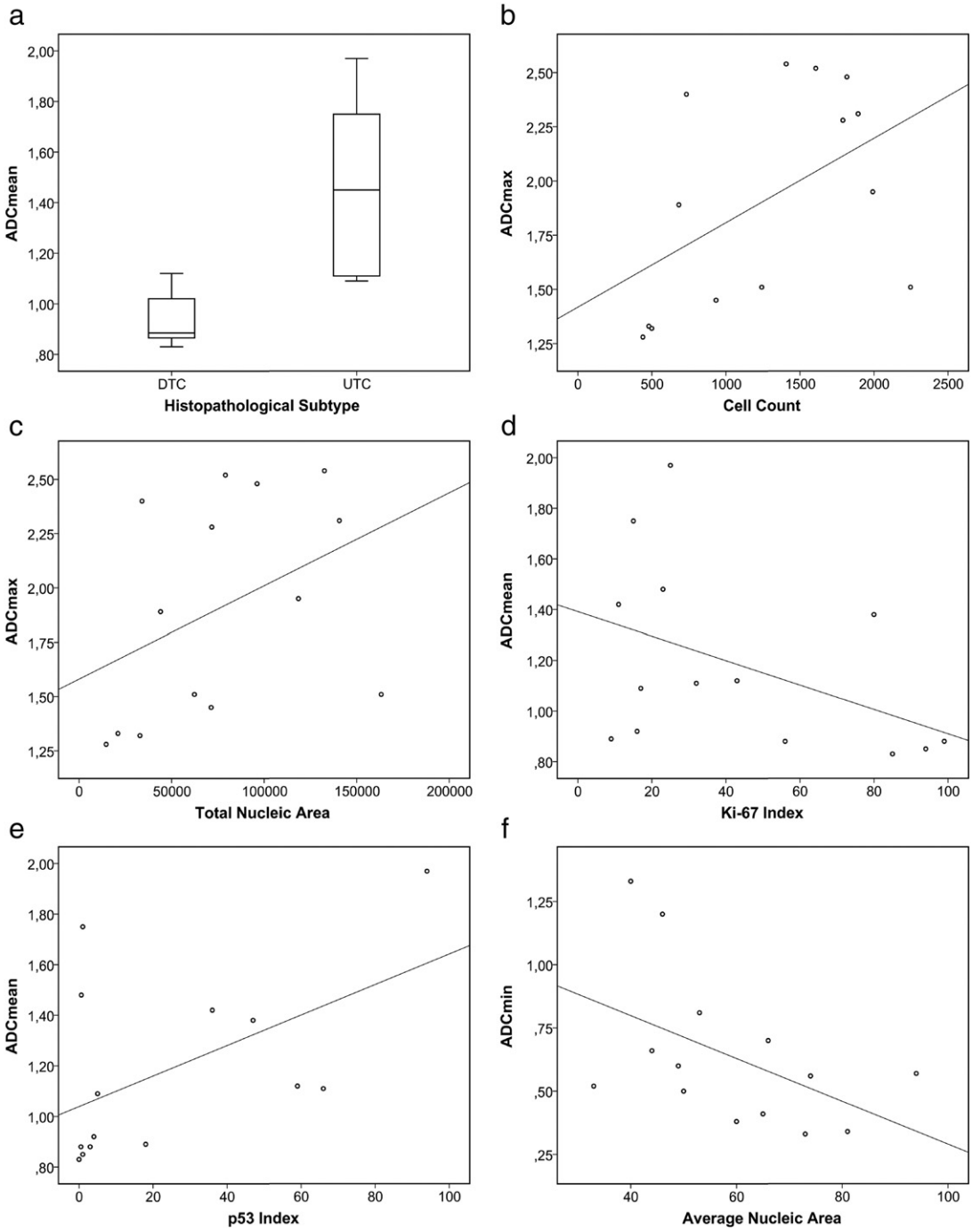


**Figure 3.** (a) ADCmean values of differentiated versus undifferentiated thyroid carcinoma. (b–f) Scatter plots graphically summarizing the relationships between DWI parameters and (immuno)histopathological properties.

separation of DTC versus UTC, as its association with Ki-67 expression underlines its relation to the proliferative activity of tumors, which is a general hallmark of cancer [35] and important for assessment of prognosis and therapy response in the clinical context.

Also, a trend of positive correlation between p53 overexpression and ADCmean was displayed in our study. p53 is one of the most important tumor suppressors controlling cell fate mainly by inducing growth arrest, apoptosis, and senescence [36]. Under normal, unstressed conditions, p53 remains undetectable because of its rapid degradation via the proteasome [36]. In case of thyroid cancer, p53 expression is associated with a good prognosis [37–39] and may be used as a marker to identify less aggressive cases of thyroid cancer that may not need aggressive management [40]. As discussed above, low ADCmean values are associated with increased cell proliferation and therefore indicate aggressive tumor biology. Also, increased expression of p53 shows an association with increased ADCmean values, which further underlines the significance of ADCmean as *in vivo* biomarker predicting tumor aggressiveness.

ADCmax showed a significant correlation with total nuclei area and cellularity in our study. Both histopathological parameters reflect areas of increased cell density. It is well known that different ADC fractions—in most cases, ADCmean; more seldomly, ADCmin—are associated with increased cellular density as a consequence of reduced extracellular space [8]. ADCmax indicates tissue areas with comparably high water diffusibility. It is therefore somewhat unexpected that ADCmax and cellularity as well as total nuclei area show a strong, significant correlation. Recent studies investigated the expression of aquaporins in thyroid carcinoma. Niu and colleagues were able to show that normal and neoplastic thyroid tissue with follicular cell origin expresses high levels of aquaporin 4—a protein physiologically forming water channels in the kidneys and the central nervous system—and therefore concluded that aquaporin 4 may play an important role for fluid homeostasis of normal and transformed follicular thyroid cells [41]. Complementarily, Lacroix and colleagues showed that aquaporin 7 is upregulated in a certain subtype of FTCs [42]. A correlation between AQP4 expression and ADCmax values has been described in other space-occupying lesions [43]. We thereupon hypothesize that, as a peculiarity, thyroid carcinoma cells of follicular cell origin, being equipped with a comparably high set of water channels that facilitate water diffusibility, show a clear association between increased water diffusion in DWI in areas of increased cellularity.

This study suffers some limitations. Firstly, it is a feasibility study and thereby only has a small number of DTC and UTC patients. A larger cohort of patients is necessary to confirm our initial findings. Secondly, no MTC cases are included in this study. Because of the rarity of MTC, no patient could be included in this investigation, and additional works must be performed to investigate if RESOLVE DWI can be helpful to distinguish between MTC, UTC, and DTC. As a third point, lack of fine-needle aspiration biopsies has to be mentioned. Fine-needle aspiration biopsies are considered a very useful diagnostic tool in thyroid cancer workup. It would be interesting to compare our DWI data with corresponding fine-needle aspiration biopsy results to understand whether MRI as noninvasive tool might provide comparable (or even superior) information to fine-needle aspiration biopsies.

## Conclusion

This study shows that ADCmean values obtained from presurgical DWI using a RESOLVE sequence at 3 T have the potential to stratify patients based on the grade of dedifferentiation of thyroid carcinoma. The results of our study demonstrate clearly decreased ADCmean values in UTC compared with DTC. Therefore, ADCmean values can aid the thyroid surgeon in the presurgical setting to preselect optimal therapeutic strategies and inform the patient about the probable extent of surgery and associated risks.

## Conflict of Interest

There are no conflicts of interest.

## References


[1] Katoh H, Yamashita K, Enomoto T, and Watanabe M (2015). Classification and general considerations of thyroid Cancer. *Ann Clin Pathol* , 1–9.

[2] Ferrari SM, Fallahi P, Politti U, Materazzi G, Baldini E, and Ulisse S, et al (2015). Molecular targeted therapies of aggressive thyroid cancer. *Front Endocrinol (Lausanne)* **6**, 176. http://dx.doi.org/10.3389/fendo.2015.00176.

[3] Nixon I (2015). The surgical approach to differentiated thyroid Cancer. *F1000Res* **4**. http://dx.doi.org/10.12688/f1000research.7002.1.

[4] Xie J, Fan Y, and Zhang X (2015). Molecular mechanisms in differentiated thyroid cancer. *Front Biosci (Landmark Ed)* **21**, 119–129.

[5] Vecchio G and Santoro M (2000). Oncogenes and thyroid cancer. *Clin Chem Lab Med* **38**, 113–116.

[6] Weber KB and McDermott MT (2006). Oncogenes in Thyroid Cancer. linkspringercom. Totowa, NJ: Humana Press; 2006 41–53. http://dx.doi.org/10.1007/978–1–59259-995-0_5.

[7] Vitale M (2011). Rethinking the role of oncogenes in papillary thyroid cancer initiation. *Front Endocrinol (Lausanne)* **3**, 83. http://dx.doi.org/10.3389/fendo.2012.00083.

[8] Chen L, Liu M, Bao J, Xia Y, Zhang J, and Zhang L, et al (2013). The correlation between apparent diffusion coefficient and tumor cellularity in patients: a meta-analysis. In: Hess CP, editor. PLoS One, 8; 2013. p. e79008. http://dx.doi.org/10.1371/journal.pone.0079008.s001.

[9] Surov A, Gottschling S, Mawrin C, Prell J, Spielmann RP, and Wienke A, et al (2015). Diffusion-weighted imaging in meningioma: prediction of tumor grade and association with histopathological parameters. TRANON. The authors. **8**, 517–523. http://dx.doi.org/10.1016/j.tranon.2015.11.012.

[10] Chen L, Zhang J, Chen Y, Wang W, Zhou X, and Yan X, et al (2014). Relationship between apparent diffusion coefficient and tumour cellularity in lung cancer. *PLoS One* **9**, e99865. http://dx.doi.org/10.1371/journal.pone.0099865.

[11] Shi HF, Feng Q, Qiang JW, Li RK, Wang L, and Yu JP (2013). Utility of diffusion-weighted imaging in differentiating malignant from benign thyroid nodules with magnetic resonance imaging and pathologic correlation. *J Comput Assist Tomogr* **37**, 505–510. http://dx.doi.org/10.1097/RCT.0b013e31828d28f0.

[12] Wu L-M, Chen X-X, Li Y-L, Hua J, Chen J, and Hu J, et al (2014). On the utility of quantitative diffusion-weighted MR imaging as a tool in differentiation between malignant and benign thyroid nodules. *Acad Radiol* **21**, 355–363. http://dx.doi.org/10.1016/j.acra.2013.10.008.

[13] Schueller-Weidekamm C, Kaserer K, Schueller G, Scheuba C, Ringl H, and Weber M, et al (2008). Can quantitative diffusion-weighted MR imaging differentiate benign and malignant cold thyroid nodules? Initial results in 25 patients. *Am J Neuroradiol* **30**, 417–422. http://dx.doi.org/10.3174/ajnr.A1338.

[14] Porter DA and Heidemann RM (2009). High resolution diffusion-weighted imaging using readout-segmented echo-planar imaging, parallel imaging and a two-dimensional navigator-based reacquisition. *Magn Reson Med* **62**, 468–475. http://dx.doi.org/10.1002/mrm.22024.

[15] Surov A, Caysa H, Wienke A, Spielmann RP, and Fiedler E (2015). Correlation between different ADC fractions, cell count, Ki-67, total nucleic areas and average nucleic areas in meningothelial meningiomas. *Anticancer Res* **35**, 6841–6846.

[16] Chiu CG, Strugnell SS, Griffith OL, Jones SJM, Gown AM, and Walker B, et al (2010). Diagnostic utility of galectin-3 in thyroid cancer. *Am J Pathol* **176**, 2067–2081. http://dx.doi.org/10.2353/ajpath.2010.090353.

[17] Hoang JK, Lee WK, Lee M, Johnson D, and Farrell S (2007). US features of thyroid malignancy: pearls and pitfalls. RadioGraphics, 27. Radiological Society of North America; 2007. p. 847–860. http://dx.doi.org/10.1148/rg.273065038 [discussion 861–5].

[18] Niu L-J, Hao Y-Z, and Zhou C-W (2006). Diagnostic value of ultrasonography in thyroid lesions. *Zhonghua Er Bi Yan Hou Tou Jing Wai Ke Za Zhi* **41**, 415–418.

[19] Wong KT and Ahuja AT (2005). Ultrasound of thyroid cancer. *Cancer Imaging* **5**, 157–166. http://dx.doi.org/10.1102/1470-7330.2005.0110.

[20] Braun B and Blank W (2005). Sonography of the neck and superior mediastinum. Internist (Berl), 46. Springer-Verlag; 2005. p. 1133–1145. http://dx.doi.org/10.1007/s00108–005–1467-9 [quiz 1146].

[21] Marcus C, Whitworth PW, Surasi DS, Pai SI, and Subramaniam RM (2014). PET/CT in the management of thyroid cancers. AJR Am J Roentgenol. American Roentgen Ray. *Society* **202**, 1316–1329. http://dx.doi.org/10.2214/AJR.13.11673.

[22] Saif MW, Tzannou I, Makrilia N, and Syrigos K (2010). Role and cost effectiveness of PET/CT in management of patients with cancer. *Yale J Biol Med* **83**, 53–65.

[23] Schlumberger M, Tubiana M, De Vathaire F, Hill C, Gardet P, and Travagli JP, et al (1986). Long-term results of treatment of 283 patients with lung and bone metastases from differentiated thyroid carcinoma. *J Clin Endocrinol Metab* **63**, 960–967. http://dx.doi.org/10.1210/jcem-63-4-960.

[24] Treglia G, Muoio B, Giovanella L, and Salvatori M (2013). The role of positron emission tomography and positron emission tomography/computed tomography in thyroid tumours: an overview. Eur Arch Otorhinolaryngol, 270. Springer-Verlag; 2013. p. 1783–1787. http://dx.doi.org/10.1007/s00405-012-2205-2.

[25] Wu Y, Yue X, Shen W, Du Y, Yuan Y, and Tao X, et al (2013). Diagnostic value of diffusion-weighted MR imaging in thyroid disease: application in differentiating benign from malignant disease. *BMC Medl Imaging* **13**, 1. http://dx.doi.org/10.1186/1471-2342-13-23.

[26] Razek AAKA, Sadek AG, Kombar OR, Elmahdy TE, and Nada N (2008). Role of apparent diffusion coefficient values in differentiation between malignant and benign solitary thyroid nodules. *Am J Neuroradiol* **29**, 563–568. http://dx.doi.org/10.3174/ajnr.A0849.

[27] Vrachimis A, Stegger L, Wenning C, Noto B, Burg MC, and Konnert JR, et al (2016). [(68)Ga]DOTATATE PET/MRI and [(18)F]FDG PET/CT are complementary and superior to diffusion-weighted MR imaging for radioactive-iodine–refractory differentiated thyroid cancer. Eur J Nucl Med Mol Imaging, 43. Springer Berlin Heidelberg; 2016. p. 1765–1772. http://dx.doi.org/10.1007/s00259-016-3378-5.

[28] Lu Y, Moreira AL, Hatzoglou V, Stambuk HE, Gonen M, and Mazaheri Y, et al (2015). Using diffusion-weighted MRI to predict aggressive histological features in papillary thyroid carcinoma: a novel tool for pre-operative risk stratification in thyroid cancer. *Thyroid* **25**, 672–680. http://dx.doi.org/10.1089/thy.2014.0419.

[29] Cabanillas ME, Dadu R, Hu MI, Lu C, Gunn GB, and Grubbs EG, et al (2015). Thyroid gland malignancies. *Hematol Oncol Clin North Am* **29**, 1123–1143. http://dx.doi.org/10.1016/j.hoc.2015.07.011.

[30] Nixon IJ, Ganly I, and Shah JP (2013). Thyroid cancer: surgery for the primary tumor. *Oral Oncol* **49**, 654–658. http://dx.doi.org/10.1016/j.oraloncology.2013.03.439.

[31] Schlüter C, Duchrow M, and Wohlenberg C (1993). The cell proliferation-associated antigen of antibody Ki-67: a very large, ubiquitous nuclear protein with numerous repeated elements, representing a new kind of cell. *J Cell* , 1–10.

[32] Schob S, Meyer J, Gawlitza M, Frydrychowicz C, Müller W, and Preuss M, et al (2016). Diffusion-weighted MRI reflects proliferative activity in primary CNS lymphoma. In: Coles JA, editor. PLoS One, 11; 2016. p. e0161386–e0161411. http://dx.doi.org/10.1371/journal.pone.0161386.

[33] Tisell LE, Oden A, Muth A, Altiparmak G, Mölne J, and Ahlman H, et al (2003). The Ki67 index a prognostic marker in medullary thyroid carcinoma. *Br J Cancer* **89**, 2093–2097. http://dx.doi.org/10.1038/sj.bjc.6601453.

[34] Pujani M, Arora B, Singh SK, and Tejwani N (2009). Role of Ki-67 as a proliferative marker in lesions of thyroid. *Indian J Cancer* **47**, 304–307. http://dx.doi.org/10.4103/0019-509X.64727.

[35] Hanahan D and Weinberg RA (2000). The hallmarks of cancer. *Cell* **100**, 57–70. http://dx.doi.org/10.1016/S0092-8674(00)81683-9.

[36] Wang Z and Sun Y (2010). Targeting p53 for novel anticancer therapy. *Transl Oncol* **3**, 1–12. http://dx.doi.org/10.1593/tlo.09250.

[37] Godballe C, Asschenfeldt P, Jørgensen KE, Bastholt L, Clausen PP, and Hansen TP, et al (1998). Prognostic factors in papillary and follicular thyroid carcinomas: p53 expression is a significant indicator of prognosis. *Laryngoscope* **108**, 243–249.

[38] Bachmann K, Pawliska D, Kaifi J, Schurr P, Zörb J, and Mann O, et al (2006). P53 is an independent prognostic factor for survival in thyroid cancer. *Anticancer Res* **27**, 3993–3997.

[39] Nishida T, Nakao K, Hamaji M, Nakahara MA, and Tsujimoto M (1996). Overexpression of p53 protein and DNA content are important biologic prognostic factors for thyroid cancer. *Surgery* **119**, 568–575.

[40] Marcello MA, Morari EC, Cunha LL, De Nadai Silva AC, Carraro DM, and Carvalho AL, et al (2013). P53 and expression of immunological markers may identify early stage thyroid tumors. *Clin Dev Immunol* **2012**, 846584. http://dx.doi.org/10.1155/2013/846584.

[41] Niu D, Kondo T, Nakazawa T, Kawasaki T, Yamane T, and Mochizuki K, et al (2011). Differential expression of aquaporins and its diagnostic utility in thyroid cancer. *PLoS One* **7**, e40770. http://dx.doi.org/10.1371/journal.pone.0040770.

[42] Lacroix L, Lazar V, Michiels S, Ripoche H, Dessen P, and Talbot M, et al (2005). Follicular thyroid tumors with the PAX8-PPARgamma1 rearrangement display characteristic genetic alterations. *Am J Pathol* **167**, 223–231.

[43] Schob S, Surov A, Wienke A, Meyer HJ, Spielmann RP, and Fiedler E (2016). Correlation between aquaporin 4 expression and different DWI parameters in grade I meningioma. *Mol Imaging Biol*. http://dx.doi.org/10.1007/s11307-016-0978-1.